

Low-energy excitations in electron-doped metal phthalocyanine from NMR in $\text{Li}_{0.5}\text{MnPc}$

M.Filibian, and P. Carretta

Department of Physics "A.Volta", University of Pavia, Via Bassi 6, I-27100, Pavia (Italy)

T. Miyake, Y. Taguchi, and Y. Iwasa

Institute for Materials Research, Tohoku University, Sendai 980-8577 (Japan)

^7Li and ^1H NMR and magnetization measurements in $\text{Li}_{0.5}\text{MnPc}$ ($\text{Pc} \equiv \text{C}_{32}\text{H}_{16}\text{N}_8$), recently proposed as a strongly correlated metal, are presented. Two different low-frequency dynamics are evidenced. The first one, probed by ^1H nuclei gives rise to a slowly relaxing magnetization at low temperature and is associated with the freezing of MnPc $S = 3/2$ spins. This dynamic is similar to the one observed in pristine $\beta\text{-MnPc}$ and originates from Li depleted chain segments. The second one, evidenced by ^7Li spin-lattice relaxation rate, is associated with the hopping of the electrons along Li-rich chains. The characteristic correlation times for the two dynamics are derived and the role of disorder is briefly discussed.

PACS numbers: 76.60.Es, 71.27.+a, 75.50.Xx

I. INTRODUCTION

Metal phthalocyanines (hereafter MPc) have attracted a lot of interest in the last decades owing to their technological applicabilities as dyes, gas sensors or in electro-optical devices¹. A renewed interest on these systems has emerged after the observation that thin films of MPc show a marked increase in the electrical conductivity once they are doped with alkali ions². In view of the similarities that alkali-doped MPc (A_xMPc) share with fullerenes, Tosatti et al. ³ have analyzed, within a model successfully applied to other strongly correlated electron systems⁴, the possibility that superconductivity could occur also in A_xMPc . It was found that strongly correlated superconductivity could develop also in A_xMPc for $x \simeq 2$, with a magnitude and a symmetry of the order parameter which would depend on the intensity of the local exchange (Hund coupling) and on Jahn-Teller coupling³. Accordingly a growing interest on these compounds has arisen in the last year. Nevertheless, the synthesis of bulk A_xMPc is non-trivial and hitherto still at a preliminary stage. So far only $\beta\text{-Li}_x\text{MnPc}$ powders have been grown in a reproducible way, for $0 \leq x \leq 4$ ⁵, and the evolution of the lattice parameters and of their basic magnetic properties with doping have been studied .

Li_xMnPc structure (Fig.1) is formed by chains along which MnPc molecules are stacked. From high-resolution X-ray diffraction it was observed that Li^+ ions stay in between adjacent molecules piling up along the chain and are tightly bound to pyrrole-bridging N atoms⁵. This one-dimensional structure is quite similar to the one of other organic conductors which have been deeply investigated in the last twenty years and are still subject of an intense research activity, the Bechgard salts⁶. Magnetization measurements carried out in Li_xMnPc , have revealed a progressive increase in the Curie constant with doping and a modification in the magnitude and sign of the superexchange coupling, a neat demonstra-

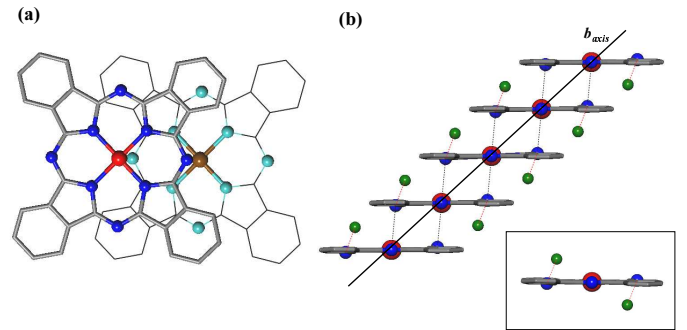


FIG. 1: (a) Projection of two neighboring MnPc molecules within the same stack along the normal direction to their planar rings in Li_2MnPc . The Mn²⁺ ions are depicted as red (brown) spheres lying directly above (below) neighboring light blue (dark blue) N atoms. (b) The slip-stacked MnPc assembly along the b axis in Li_2MnPc . Li^+ ions (depicted in green) are disordered and reside exclusively in the intrastack spacing and bond strongly to pyrrole-bridging N atoms (red dotted lines). The inset shows the Li_2MnPc building block of the 1D assemblies.

tion that electrons are transferred to MPc molecular orbitals. In order to study the modifications of the microscopic electronic properties of Li_xMnPc with doping, one can conveniently use local probes as ^7Li and ^1H nuclei. In the following we present a ^7Li and ^1H nuclear magnetic resonance (NMR) and magnetization study of $\text{Li}_{0.5}\text{MnPc}$. From nuclear spin-lattice relaxation measurements two different dynamics were found. A low-frequency dynamics associated with the progressive freezing of MnPc $S = 3/2$ spins and a dynamics at much higher frequency of diffusive character. The characteristic correlation times, the hyperfine couplings and the

temperature and time evolution of the macroscopic magnetization are estimated and discussed in the light of the possible evolution of the molecular electronic and spin configuration. The experimental results are presented in the following sections. Section III is dedicated to their analysis and discussion, while the final conclusions are presented in Sect. IV.

II. TECHNICAL ASPECTS AND EXPERIMENTAL RESULTS

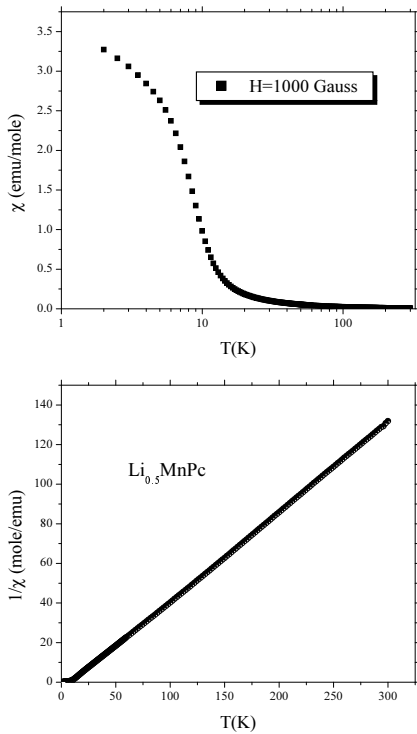


FIG. 2: (top) Temperature dependence of the susceptibility, defined as $\chi = M/H$, in $\text{Li}_{0.5}\text{MnPc}$ for $H = 1$ kGauss. (bottom) Temperature dependence of the inverse of the susceptibility. One can notice that for $T \geq 15$ K Curie-Weiss law is obeyed.

As-purchased MnPc powder was purified by vacuum sublimation prior to the intercalation procedure. Li-intercalation was carried out by using liquid-phase process in an Ar-filled glove box. Details of the sample preparation procedures are described in Ref. 5. The powder samples were then sealed in a quartz tube to avoid oxidation.

Magnetization measurements were performed using a Quantum Design XPMS-XL7 SQUID magnetometer. At high temperatures, above 15 K, the magnetization M was found to increase linearly with the field intensity H and hence the susceptibility can be defined from $\chi = M/H$. One observes (Fig.2) a high temperature Curie-

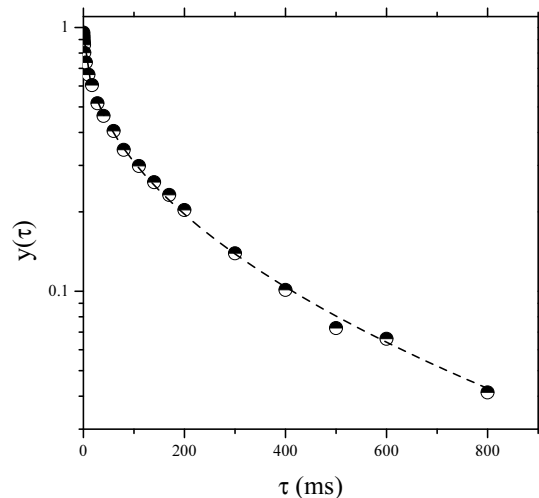


FIG. 3: Recovery law for ${}^7\text{Li}$ nuclear magnetization after a saturating pulse sequence. The dashed line is the best fit according to $y(\tau) = \exp(-(\tau/T_1)^\beta)$

Weiss behaviour

$$\chi = \frac{C}{T - \Theta} + \chi_o, \quad (1)$$

with $C = 2.27$ emu.K/mole Curie constant and $\Theta = 7.8 \pm 0.2$ K, indicating a dominant ferromagnetic coupling. χ_o is the sum of Van-Vleck and diamagnetic contributions, which are assumed weakly temperature dependent⁷. Below about 10 K a clear departure from Curie-Weiss law is observed. The magnetization shows an upturn, is no longer linear in the field and is observed to slowly relax in time, a behaviour suggesting a freezing of the molecular spins. This behaviour is reminiscent of the one observed in pure $\beta\text{-MnPc}$ ⁵.

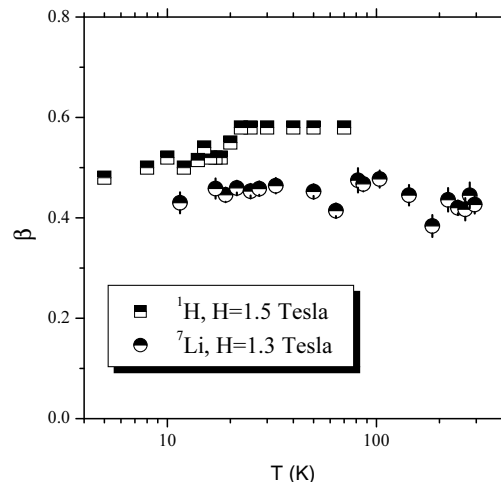


FIG. 4: Temperature dependence of the stretched exponential exponent β for ${}^7\text{Li}$ and for the fast component of ${}^1\text{H}$ recovery laws.

NMR measurements were performed by using standard radiofrequency (RF) pulse sequences. ${}^7\text{Li}$ and ${}^1\text{H}$ powder spectra were obtained from the Fourier transform of

half of the echo signal after a $\pi/2 - \tau - \pi/2$ pulse sequence. The spectra were observed to be Gaussian with a linewidth increasing upon cooling, as the macroscopic susceptibility. In ${}^7\text{Li}$ ($I = 3/2$) spectra there was no clear evidence of the satellite transitions, which are much less intense than the central one. Moreover, we observed that the length of the $\pi/2$ pulse was about half of that derived for ${}^7\text{Li}$ in an aqueous solution of LiCl, where all transitions are irradiated. This indicates that practically just the central $m_I = 1/2 \leftrightarrow -1/2$ transition of ${}^7\text{Li}$ was irradiated. The echo intensity $E(2\tau)$ was observed to decrease upon increasing τ following an almost Gaussian law, with a characteristic decay time for ${}^7\text{Li}$ around $T_2^G \simeq 165\mu\text{s}$, while $\simeq 45\mu\text{s}$ for ${}^1\text{H}$, around 100 K. Finally, the relative intensity of ${}^7\text{Li}$ and ${}^1\text{H}$ signals for $\tau \rightarrow 0$ was observed to be consistent with a Li content of 0.50 ± 0.01 per formula unit, in excellent agreement with the expected nominal doping.

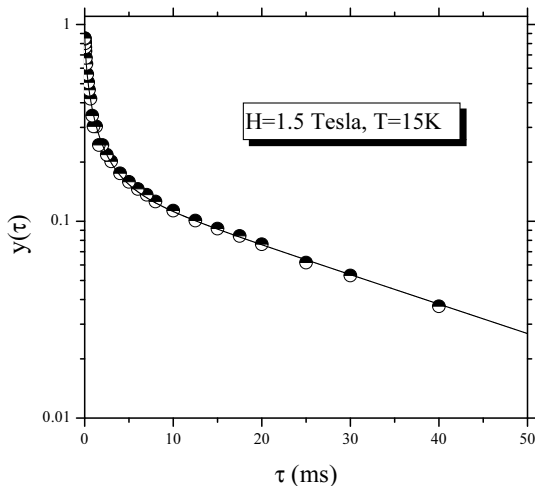


FIG. 5: Recovery law for ${}^1\text{H}$ nuclear magnetization after a saturating pulse sequence. The solid line is the best fit according to Eq.2

Nuclear spin-lattice relaxation rate $1/T_1$ was estimated from the recovery of nuclear magnetization $m(\tau)$ after a saturating RF pulse sequence. The recovery law of ${}^7\text{Li}$ was observed to be a stretched exponential (Fig. 3), namely $y(\tau) \equiv 1 - m(\tau)/m(\tau \rightarrow \infty) = \exp(-(\tau/T_1)^\beta)$, with $\beta \simeq 0.45$ over all the temperature range (Fig. 4). A stretched exponential recovery indicates the presence of disorder at the microscopic level. Also ${}^1\text{H}$ recovery law was essentially of stretched exponential character, however, for large delays τ a clear departure from a simple stretched exponential recovery was noticed. The recovery could be nicely fit according to (Fig. 5)

$$y(\tau) = A e^{-(\frac{\tau}{T_1})^\beta} + (1 - A) e^{-(\frac{\tau}{T_1})} \quad (2)$$

with $A \simeq 0.8$ and $\beta \simeq 0.5$ over the explored temperature range (Fig. 4). The temperature dependence of ${}^7\text{Li}$ and ${}^1\text{H}$ relaxation rates derived from the aforementioned recovery laws are shown in Figs. 6 and 8. At temperatures above 35 K ${}^1\text{H}$ relaxation rate $1/T_1^s$ shows

a low-frequency divergence with $1/T_1^s \propto 1/\sqrt{H}$ (Fig. 7), a behaviour which is typical of one-dimensional spin systems.

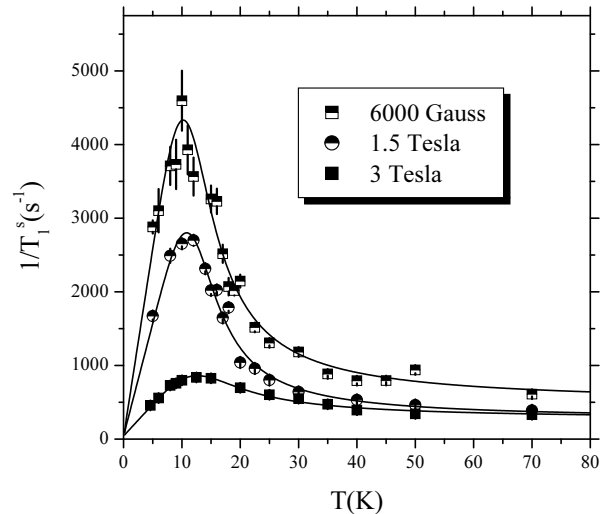


FIG. 6: Temperature dependence of ${}^1\text{H}$ $1/T_1^s$ at different magnetic fields. The solid lines are the best fit according to Eq.8, for $\langle E_A \rangle \simeq \Delta = 25$ K.

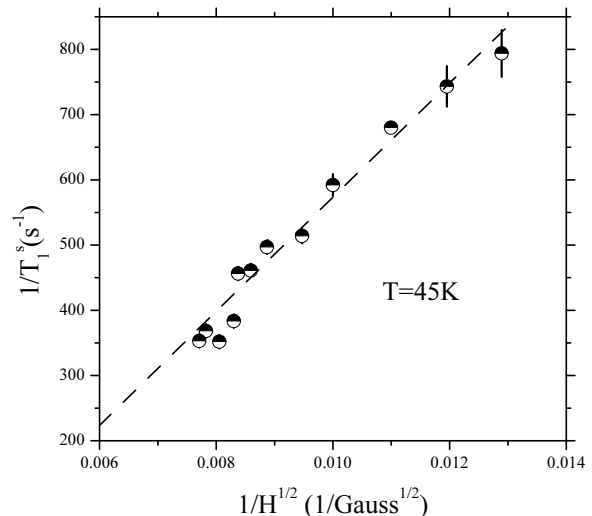


FIG. 7: ${}^1\text{H}$ nuclear spin-lattice relaxation rate $1/T_1^s$, at $T = 45$ K, reported as a function of $1/\sqrt{H}$ in order to evidence the diffusive nature of the spin correlations. The dashed line is the best fit according to Eq. 6 in the text.

III. DISCUSSION

The temperature dependence of the magnetic susceptibility is characteristic of ferromagnetically correlated spin chains, as observed for pristine $\beta\text{-MnPc}$. The fit of the susceptibility according to Curie-Weiss law yields $\Theta = 7.5$ K, corresponding to an exchange coupling constant $J = \Theta/[2z\sqrt{S(S+1)/3}] \simeq 1.7$ K, for $S = 3/2$ and taking $z = 2$ for the number of nearest neighbours. This value of Θ is lower than the one of pure $\beta\text{-MnPc}$,

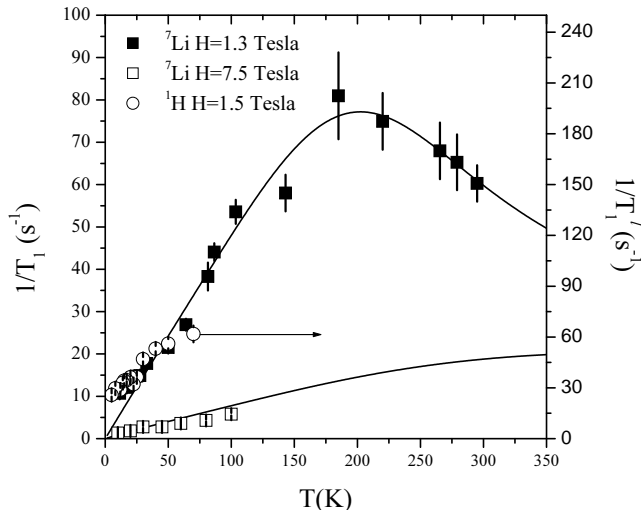


FIG. 8: Temperature dependence of ${}^7\text{Li}$ $1/T_1$ (squares) and of ${}^1\text{H}$ $1/T_1^l$ (circles and right vertical scale), the relaxation rate of the slowly relaxing component of ${}^1\text{H}$ magnetization (see Fig.5). The solid lines are the best fit according to Eq.8, for $< E_g > \simeq \Delta = 410$ K.

whereas the Curie constant is larger in $\text{Li}_{0.5}\text{MnPc}$, in agreement with the results reported by Taguchi et al. 5 for $0 \leq x \leq 4$ who observed that for $x \rightarrow 2$ Curie constant tends to the one expected for $S = 5/2$ with $g = 2$, while Θ becomes negative, i.e. the chain becomes antiferromagnetically correlated.

β -MnPc in its ground-state has a completely filled a_{1u} level, a half-filled a_{1g} level and two degenerate half-filled $1e_g$ levels^{7,8}. In order to attain an $S = 5/2$ molecular spin state upon increasing Li content it is necessary to start filling the upper energy levels, as the two-fold degenerate $2e_g(\pi)$ LUMO and the $b_1(d_{x^2-y^2})$ states. A scenario which differs from the one of MPC containing transition metal ions with more d-electrons than Mn^{2+} . In fact, in FePc and CoPc Hund rule is not obeyed and the other electrons occupy the $1e_g$ levels, so that one has an $S = 1$ and an $S = 1/2$ configuration, respectively. Taking into account the crystal-field modifications induced by Li^+ , the $S = 5/2$ state could in principle result from two different configurations. As suggested in Ref.5, Li^+ gives rise to a more isotropic crystal-field and the energy of the LUMO and $b_1(d_{x^2-y^2})$ can be lowered, so that an electron can be promoted from the a_{1u} to the $b_1(d_{x^2-y^2})$ level, in accordance to Hund's rule. Then the $S = 5/2$ state would result from the occupancy of all d -character orbitals. The electrons injected by Li doping, which fill $2e_g(\pi)$ LUMO, would not contribute to the total molecular spin once they form a singlet state, a situation similar to the one observed in the fullerenes⁹. Singlet formation can occur if Jahn-Teller coupling for the $2e_g(\pi)$ state with the B_{1g} and B_{2g} β -MnPc vibrational modes is larger than its Hund coupling³.

On the other hand, an $S = 5/2$ state is also consistent with a triplet state for the electrons on the LUMO, provided that $b_1(d_{x^2-y^2})$ energy is not significantly lowered by Li doping and this latter level remains empty.

The comprehension of which one of the two configurations is actually taking place is important, as it will allow to know which one of the two couplings, Jahn-Teller or Hund's, is dominant for the electrons on the LUMO and then, in case strongly correlated superconductivity would develop, the symmetry of the superconducting order parameter. Nevertheless, from our measurements alone it is not possible to discern among the two scenarios. Crystal-field calculations and microscopic techniques using Mn^{2+} ions as probes (e.g. EPR), would allow to clarify this aspect. It is noticed that the filling of the LUMO, which overlaps with the a_{1g} orbitals of adjacent molecules along the chain, can induce antiferromagnetic correlations¹⁰, which would explain the change of sign of Curie-Weiss temperature with increasing doping.

Now, the configuration with two Li^+ ions close to an MnPc molecule gives rise to a crystal-field which decrease the energy of the b_1 states and also of the LUMO. Accordingly, one should expect that the energy of $S = 5/2$ state is possibly lower than the one of $S = 2$ and $S = 3$ states, associated with one unpaired electron on the LUMO. Then, it is likely that the progressive increase in the Curie constant, upon increasing Li content from $x = 0$ to 2, actually originates from the contribution of $S = 3/2$ and of $S = 5/2$ chain segments, which are characterized by a more stable spin configuration. Although from magnetization data alone one cannot say if both spin configurations coexist at the microscopic level, we remark that Li_xMnPc susceptibility data can be fit with $\chi = (x/2)\chi_{Li_2} + [(2-x)/2]\chi_{Li_0}$, for $T \gg 10$ K, where the $\chi_{Li_{x=0,2}}$ susceptibility are the ones derived by Taguchi et al.⁵ for $x = 0$ and $x = 2$. As will be pointed out later on, this interpretation is corroborated by the observation of two different dynamics in nuclear spin-lattice relaxation measurements.

At low temperature one observes a deviation from Curie-Weiss law which, however, is not associated with a three-dimensional long-range order. In fact, one observes a slowly relaxing magnetization at low temperature which suggests a progressive freezing of the molecular spins, a scenario observed in other spin chains characterized by a sizeable magnetic anisotropy¹¹. At a temperature of 3 K the magnetization was observed to recover its equilibrium value, after increasing the field from 0 to 1 Tesla, in a characteristic time $\tau_M \simeq 1050$ s. This macroscopic relaxation has to be associated with the long-wavelength $q \rightarrow 0$ modes. One can compare this result with the average relaxation time measured by means of AC-susceptibility by Taguchi et al. 5. From the peak in the imaginary part of the AC-susceptibility measured at different frequencies one can roughly estimate an average correlation time $\tau_{AC} \simeq 10^{-10} \exp(90/T)$ s, corresponding to $\tau_{AC} \simeq 1070$ s at 3 K, in rather good agreement with the value estimated from the relaxation of the magnetization.

Now we turn to the analysis of the low-energy excitations in the light of nuclear spin-lattice relaxation rate $1/T_1$ measurements. In the presence of a magnetic relax-

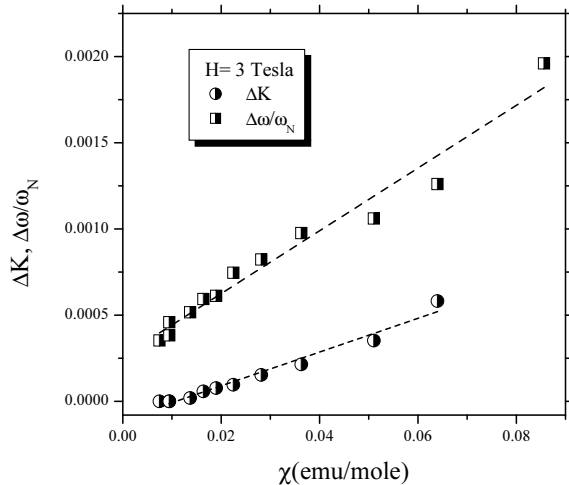


FIG. 9: ^1H paramagnetic shift ΔK (see Eq.4) and normalized line broadening $\Delta\omega/\omega_N$ reported as a function of the magnetic susceptibility measured with the SQUID magnetometer, with the temperature as an implicit parameter. The dashed lines evidence the linear dependence of the line broadening and of the shift on the susceptibility (see Eq.4).

ation mechanism

$$\frac{1}{T_1} = \frac{\gamma^2}{2} \int_{-\infty}^{+\infty} e^{i\omega_N t} \langle h_+(t)h_-(0) \rangle dt, \quad (3)$$

where h_{\pm} are the transverse components of the hyperfine field at the nucleus, ω_N nuclear resonance frequency and γ the nuclear gyromagnetic ratio. For localized spins one has that $\vec{h}(t) = \sum_i \tilde{A}_i \vec{S}_i(t)$, with \tilde{A}_i the hyperfine coupling between the i -th electron spin and the nucleus. In a single crystal the magnitude of the hyperfine coupling can be estimated from the shift of the resonance frequency ω_N with respect to the nuclear Larmor frequency ω_o in the applied magnetic field. In fact, one can write

$$\frac{\omega_N - \omega_o}{\omega_o} \equiv \Delta\tilde{K} = \frac{\tilde{A}_T \tilde{\chi}}{g\mu_B N_A} \quad (4)$$

where the macroscopic susceptibility $\tilde{\chi}$, the hyperfine coupling $\tilde{A}_T = \sum_i \tilde{A}_i$ and the shift $\Delta\tilde{K}$ are all tensors, in principle. Therefore, in a powder one should observe an effective broadening of the line rather than a shift. Indeed both for ^1H and ^7Li one observes that the line broadens with increasing χ (Figs. 9 and 10). The line shape is Gaussian for both nuclei and no structure associated with the form of the shift tensor can be discerned. Therefore, by plotting the line broadening $\Delta\omega$ vs. χ , with the temperature as an implicit parameter, one can estimate an effective coupling constant A . For both nuclei one finds $A \simeq 100$ Gauss, which is of the order of magnitude of the dipolar hyperfine field generated by the localized spins. It is noticed that ^1H spectra shows also a slight shift on cooling (Fig. 9), still proportional to χ and yielding an isotropic hyperfine coupling constant still around 100 Gauss.

In the high temperature limit $T \gg J$ the spins are uncorrelated and, in the absence of diffusive processes,

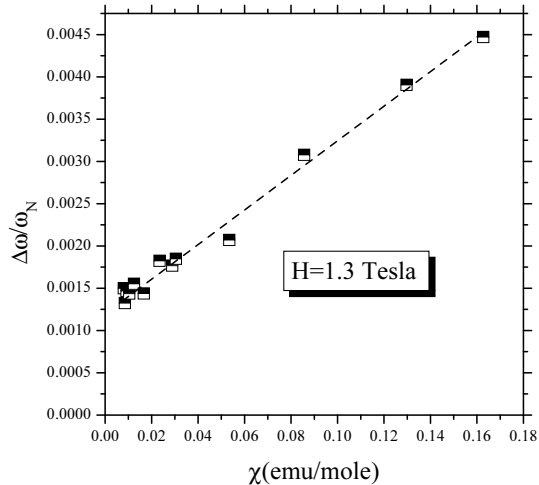


FIG. 10: ^7Li normalized line broadening $\Delta\omega/\omega_N$ reported as a function of the magnetic susceptibility measured with the SQUID magnetometer, with the temperature as an implicit parameter.

one would expect a temperature and field independent $1/T_1$, with¹²

$$\frac{1}{T_1} = \gamma^2 A^2 \frac{S(S+1)}{3} \frac{\sqrt{2\pi}}{\omega_H} \quad (5)$$

where $\omega_H = (2zJ/k_B)\sqrt{S(S+1)/3}$ is the Heisenberg exchange frequency. Accordingly ^1H $1/T_1$ is estimated around 23 s^{-1} and ^7Li $1/T_1$ around 3.5 s^{-1} , for $T \gg \Theta$. However, one notices that for $T \gg 10 \text{ K}$ ^1H $1/T_1^s$ is at least an order of magnitude larger than expected, moreover, it is strongly field dependent (Figs. 6 and 7). The marked field dependence of $1/T_1^s$ for $T \gg \Theta$ can be associated with the diffusive character of the spin correlations, which in one-dimension give rise to a $1/\sqrt{H}$ low-frequency divergence in the spectral density¹². In fact, by neglecting low-frequency cutoffs, one can write

$$\frac{1}{T_1} = \gamma^2 A^2 \frac{S(S+1)}{3} \frac{1}{\sqrt{2D}} \frac{1}{\sqrt{\omega_N}}. \quad (6)$$

By fitting the data in Fig.7 with the above equation one estimates a diffusion constant $D \simeq 1.2\omega_H$, of the right order of magnitude. It is noticed that upon cooling, for $T \rightarrow \Theta$, $1/T_1^s$ rapidly increases and then shows a broad maximum around 10 K. The amplitude of the maximum is strongly field dependent and is not associated with a three-dimensional ordering, but rather signals a low-frequency dynamics at frequencies of the order of $\omega_N \ll \omega_H$. This maximum should not be confused with the one due to soliton excitations observed in some one-dimensional ferromagnets for $T \ll J$, which would cause a completely different magnetic field dependence of $1/T_1$ ¹³. This low-frequency dynamic should rather be ascribed to the progressive freezing of the molecular spins, as detected by means of AC susceptibility in the pristine $\beta\text{-MnPc}^5$. It should be remarked that a slowing down of the frequency of the spin fluctuations to the MHz range at

$T > \Theta$ can occur only if the magnetic anisotropy barrier $E_A = DS_z^2 \geq \Theta$ and overcomes the thermal energy $k_B T$, a situation which is similar to the one of single molecule magnetic clusters¹⁴ and which was observed also in α -FePc¹⁰.

Now, if one assumes that the decay of the correlation function involving the transverse components of the hyperfine field $\langle h_+(t)h_-(0) \rangle = \langle \Delta h_{\perp}^2 \rangle \exp(-t/\tau_c)$, with $\langle \Delta h_{\perp}^2 \rangle \simeq 2A^2 S(S+1)/3$, from Eq.3 one derives

$$\frac{1}{T_1} = \frac{\gamma^2}{2} \langle \Delta h_{\perp}^2 \rangle \frac{2\tau_c}{1 + \omega_N^2 \tau_c^2}. \quad (7)$$

Taking into account that the molecular anisotropy yields an effective energy barrier E_A , which in principle can be slightly temperature dependent owing to the T-dependence of the in-chain correlation length, one can write $\tau_c = \tau_o \exp(E_A/T)$ (E_A in Kelvin). If we try to fit ^1H $1/T_1^s$ data by taking this expression for τ_c in Eq.7 we obtain a poor fit. In fact, the broad maximum in $1/T_1^s$ indicates a distribution of correlation times. For simplicity we consider a distribution of relaxation times associated with a rectangular distribution of activation energies from $\langle E_A \rangle - \Delta$ to $\langle E_A \rangle + \Delta$. Then the average relaxation time turns out¹⁵

$$\frac{1}{T_1} = \frac{\gamma^2 \langle \Delta h_{\perp}^2 \rangle T}{2 \omega_N \Delta} \left[\text{atan} \left(\omega_N \tau_o e^{\frac{\langle E_A \rangle + \Delta}{T}} \right) - \text{atan} \left(\omega_N \tau_o e^{\frac{\langle E_A \rangle - \Delta}{T}} \right) \right]. \quad (8)$$

A good fit of the data for different magnetic fields is obtained for $\tau_o = (1 \pm 0.4) \times 10^{-10}$ s and $\langle E_A \rangle \simeq \Delta \simeq 25$ K $> \Theta$, as expected for a freezing of MnPc spins. It should be remarked that this activation energy is quite different from the one (about 90 K) derived from the analysis of AC susceptibility data. Since $1/T_1$ probes the q -integrated spin susceptibility¹⁶, this observation would indicate a more rapid softening of the $q = 0$ modes with respect to the other Brillouin zone modes.

Now we turn to the discussion of ^7Li $1/T_1$. If one considers that the order of magnitude of the hyperfine coupling of ^7Li , derived from the line broadening (Fig. 10), is the same of ^1H , one would expect also a peak in ^7Li $1/T_1$ around 10 K. Remarkably, ^7Li $1/T_1$ does not show any peak, decreases upon cooling and is much smaller than $1/T_1^s$ (see Figs. 6 and 8). On the other hand, this temperature dependence is close to the one observed for $1/T_1^l$ the slowly relaxing component of ^1H magnetization (Fig.8).

The absence of a low-temperature peak in ^7Li $1/T_1$ cannot be due to a filtering of the spin excitations at the critical wave-vector, as Li is not in a symmetric position with respect to Mn ions¹⁶, moreover $1/T_1$ starts decreasing at $T \gg J$. Therefore, it is likely that in $\text{Li}_{0.5}\text{MnPc}$ two different microscopic configurations are present: Li-rich chain segments and Li depleted segments. The latter ones are characterized by a spin dynamics similar to the one of pristine β -MnPc which is evidenced by $1/T_1^s$,

while the former regions show a quite different dynamics evidenced by ^7Li $1/T_1$ and ^1H $1/T_1^l$. The coexistence of two different types of chains is consistent with the analysis of the magnetization data. It is worth to mention that from high-resolution X-ray diffraction there is no evidence of a macroscopic segregation in Li-rich and Li-depleted phases⁵, pointing out that the two configurations should coexist at the microscopic level.

At high temperature, around 180 K, ^7Li $1/T_1$ shows a broad maximum (Fig. 9). One could argue that this maximum is analogous to the one observed in $1/T_1^s$ at low temperature and that it could arise from a spin freezing. However, at variance with what is found at $T \simeq 10$ K, no evidence of a spin freezing around 200 K is present in the magnetization data (see Fig.2). Another mechanism that could give rise to a maximum in ^7Li $1/T_1$ is Li diffusion, with a hopping frequency reaching the MHz range around 200 K. However, if this was the case ^7Li NMR linewidth should be much narrower and should not follow the same temperature dependence of the macroscopic susceptibility (Fig. 10). Moreover, if Li was diffusing one should not observe a stretched exponential recovery of nuclear magnetization with a temperature-independent exponent β (Fig. 4). Therefore, ^7Li relaxation should originate from a different mechanism.

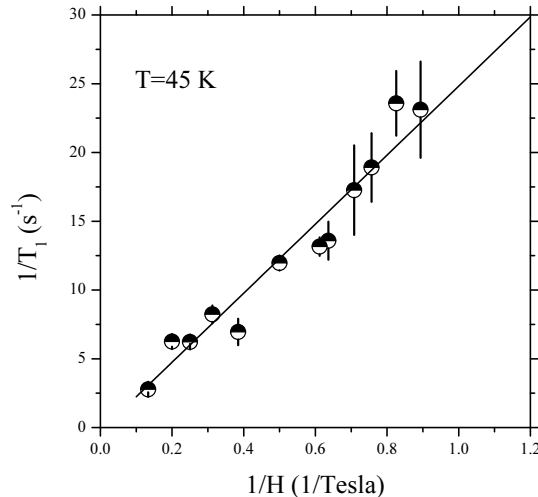


FIG. 11: ^7Li nuclear spin-lattice relaxation rate, at $T = 45$ K, reported as a function of $1/H$. The solid line shows the behaviour expected from Eq.8 for $\langle E_g \rangle = \Delta_g = 410$ K .

In Li-rich chain segments the electrons should start filling the $2e_g(\pi)$ orbitals, which overlap with the orbitals of adjacent molecules to form a one-dimensional band^{3,8}. Nevertheless, the electron delocalization can be prevented both by a strong Coulomb repulsion, as well as by the disorder associated with a non-uniform Li distribution. Accordingly, an effective gap between localized and itinerant states develops. Moreover, one should consider that the interaction of the electrons with localized spins can yield to spin-polarons formation. In this scenario one can ascribe to the electron a phenomenological¹⁷ hopping time $\tau_e = \tau_e^0 \exp(E_g/T)$, with τ_e^0 renormalized with respect to its bare value $\tau_e^0 \simeq \hbar/W$ (W the bandwidth) ow-

ing to spin-polaron formation and other effects¹⁸, while E_g is an effective gap between localized and delocalized states. The disorder, already evidenced by the stretched exponential recovery, causes a distribution of E_g 's. If one assumes a rectangular distribution of E_g 's one obtains again an expression for $1/T_1$ as in Eq.8. It is noticed that for a width of the distribution of the order of its average value (i.e. $\langle E_g \rangle \simeq \Delta_g$), at low temperature $1/T_1 \propto T$. Although this temperature dependence is the same one expected for a metal, here it has quite a different origin. Moreover, while in a one-dimensional metal $1/T_1$ should be either frequency independent or increase as $1/\sqrt{H}$ ¹⁹, from Eq.8 $1/T_1$ should increase as $1/\omega_N \propto 1/H$, at low temperature. We find that the temperature and magnetic field dependence of $1/T_1$ can be accounted for Eq.8 with $\langle E_g \rangle \simeq \Delta_g \simeq 410$ K and a $\tau_e^0 \simeq 3 \times 10^{-10}$ sec (see Figs. 8 and 11). Although it is not easy to give a definite statement in favour of this relaxation mechanism on the basis of our data alone, we point out that this phenomenological model for the electron diffusion along the chain can satisfactorily explain all ⁷Li NMR data. A homogeneous Li distribution or, in other terms, less disorder would possibly allow to observe a metallic behaviour in Li_xMnPc .

IV. CONCLUSIONS

From NMR measurements we have addressed the study of the modifications of the microscopic properties of β -

MnPc upon doping with alkali-ions. We have observed that in $\text{Li}_{0.5}\text{MnPc}$ two different dynamics coexist at the microscopic level. A first one arising from the freezing of MnPc spins, which is similar to the one observed in the undoped compound and is associated with Li depleted regions. A second one, characteristic of Li-rich regions, associated with the hopping of the electrons along the chain, whose delocalization is hindered by the disorder, the Coulomb and spin interaction. The temperature dependence of the characteristic correlation time for each one of these two processes was derived and compared to the one obtained from macroscopic techniques. These phthalocyanines could possibly become metallic for Li contents $x=2$ and $x=4$, where Li_xMnPc show a more homogeneous distribution of the Li ions and less disorder is present.

Acknowledgements

This work was supported by PRIN2004 National Project "Strongly Correlated Electron Systems with Competing Interactions" and by Fondazione CARIPO 2005 Scientific Research funds.

-
- ¹ see for example *The Porphyrin Handbook, Vol. 19: Applications of Phthalocyanines*, edited by K.M. Kadish, K.M. Smith and R. Guilard (Academic Press, 2003); *Phthalocyanines: Properties and Applications*, edited by C.C. Leznoff and A.B.P. Lener (VCH Publishers, New York, 1966) Vol.4
- ² M.F. Craciun, S.Rogge, M.J.L. den Boer, S. Margadonna, K.Prassides, Y.Iwasa And A.F. Morpurgo, *Adv. Mat.* 18, 320(2006)
- ³ E. Tosatti, M. Fabrizio, J. Tóbiak and G.E. Santoro, *Phys. Rev. Lett.* 93, 117002 (2004)
- ⁴ M. Capone, M. Fabrizio, C. Castellani, and E. Tosatti, *Phys. Rev. Lett.* 93, 047001 (2004).
- ⁵ Y. Taguchi, T. Miyake, S. Margadonna, K. Kato, K. Prassides and Y. Iwasa, *J. Am. Chem. Soc.* 128, 3313(2006)
- ⁶ D. Jérôme and H.J.Schulz, *Adv. Phys.* 31, 299 (1982)
- ⁷ C.G. Barraclough, R.L. Martin, S. Mitra and R.C. Sherwood, *J. Chem. Phys.* 53, 1638 (1970)
- ⁸ M. S. Liao and S. Scheiner, *J. Chem. Phys.* 114, 9780 (2001)
- ⁹ L. Forro and L. Mihaly, *Rep. Prog. Phys.* 64, 649 (2001)
- ¹⁰ M. Evangelisti, J. Bartolomé, L. J. de Jongh and G. Filoti, *Phys. Rev. B* 66, 144410 (2002)
- ¹¹ L. Bogani, A. Caneschi, M. Fedi, D. Gatteschi, M. Massi, M. A. Novak, M. G. Pini, A. Rettori, R. Sessoli and A. Vindigni *Phys. Rev. Lett.* 92, 207204 (2004)
- ¹² H. Benner and J. P. Boucher, in *Magnetic Properties of Layered Transition Metal Compounds*, Ed. L.J. de Jongh (Kluwer Academic Pub. 1990), p. 323
- ¹³ F. Ferraro, D. Gatteschi, A. Rettori and M. Corti, *Mol. Phys.* 85, 1073 (1995)
- ¹⁴ A. Lascialfari, Z. H. Jang, F. Borsa, P. Carretta, and D. Gatteschi *Phys. Rev. Lett.* 81, 3773 (1998)
- ¹⁵ M. Corti, S. Marini, A. Rigamonti, F. Tedoldi, D. Capsoni and V. Massarotti, *Phys. Rev. B* 56, 11056 (1997)
- ¹⁶ A. Rigamonti, F. Borsa and P. Carretta, *Rep. Progr. Phys.* 61, 1367 (1998)
- ¹⁷ P. Carretta, M. Corti and A. Rigamonti, *Phys. Rev. B* 48, 3433 (1993)
- ¹⁸ L. Zuppiroli, M. N. Bussac, S. Paschen, O. Chauvet, and L. Forro, *Phys. Rev. B* 50, 5196 (1994); M. M. Fogler, S. Teber and B. I. Shklovskii, *Phys. Rev. B* 69, 035413 (2004)
- ¹⁹ G. Soda, D. Jérôme, M. Weger, J. M. Fabre and L. Giral, *Solid State Comm.* 18, 1417 (1976); P. Carretta, C. Berthier, M. Horvatić, Y. Fagot-Revurat, P. Ségransan, D. Jérôme and C. Bourbonnais, in *Physical Phenomena at High Magnetic Fields-II*, Eds. Z. Fisk, Lev Gorkov, D. Melzer and R. Schriber (World Scientific 1996), p. 328